ARTICLE IN PRESS

BMB Reports - Manuscript Submission

Manuscript Draft

Manuscript Number: BMB-22-021

Title: Casein kinase 2 promotes the TGF-β-induced activation of α-tubulin acetyltransferase 1 in fibroblasts cultured on a soft matrix

Article Type: Article

Keywords: TGF-β; Casein kinase 2; Microtubule acetylation; α-tubulin acetyltransferase 1; Extracellular matrix

Corresponding Author: Sangmyung Rhee

Authors: Eunae You[1,#], Jangho Jeong[1,#], Jieun Lee[1], Seula Keum[1], Ye Eun Hwang[1], Jee-Hye Choi[1,#], Sangmyung Rhee[1,*,#]

Institution: [1]Department of Life Science, Chung-Ang University, Seoul, 06974, Republic of Korea,

UNCORRECTED PROOF

ARTICLE IN PRESS

Manuscript Type: Article

Title: Casein kinase 2 promotes the TGF-β–induced activation of α-tubulin acetyltransferase 1 in fibroblasts cultured on a soft matrix

Authors' names: Eunae You[1§], Jangho Jeong[1§], Jieun Lee[1], Seula Keum[1], Ye Eun Hwang[1], Jee-Hye Choi[1*] and Sangmyung Rhee[1*]

Affiliation: [1]Department of Life Science, Chung-Ang University, Seoul, 06974, Republic of Korea

[§]These authors contributed equally to this work.

Running Title: Regulation of α-TAT1 activity by CK2

Keywords: TGF-β, Casein kinase 2, Microtubule acetylation, α-tubulin acetyltransferase 1, Extracellular matrix

Corresponding Authors' Information:

Sangmyung Rhee

Tel: +82-2-820-5818; Fax: +82-2-825-5206; E-mail: sangmyung.rhee@cau.ac.kr

Jee-Hye Choi

Tel: +82-2-814-3997; Fax: +82-2-825-5206; E-mail: choijh97@cau.ac.kr

UNCORRECTED PROOF

ABSTRACT

Cell signals for growth factors depend on the mechanical properties of the extracellular matrix (ECM) surrounding the cells. Microtubule acetylation is involved in the transforming growth factor (TGF)-β–induced myofibroblast differentiation in the soft ECM. However, the mechanism of activation of α-tubulin acetyltransferase 1 (α-TAT1), a major α-tubulin acetyltransferase, in the soft ECM is not well defined. Here, we found that casein kinase 2 (CK2) is required for the TGF-β–induced activation of α-TAT1 that promotes microtubule acetylation in the soft matrix. Genetic mutation and pharmacological inhibition of CK2 catalytic activity specifically reduced microtubule acetylation in the cells cultured on a soft matrix rather than those cultured on a stiff matrix. Immunoprecipitation analysis showed that CK2α, a catalytic subunit of CK2, directly bound to the C-terminal domain of α-TAT1, and this interaction was more prominent in the cells cultured on the soft matrix. Moreover, the substitution of alanine with serine, the 236th amino acid located at the C-terminus, which contains the CK2-binding site of α-TAT1, significantly abrogated the TGF-β–induced microtubule acetylation in the soft matrix, indicating that the successful binding of CK2 and the C-terminus of α-TAT1 led to the phosphorylation of serine at the 236th position of amino acids in α-TAT1 and regulation of its catalytic activity. Taken together, our findings provide novel insights into the molecular mechanisms underlying the TGF-β–induced activation of α-TAT1 in a soft matrix.

UNCORRECTED PROOF

ARTICLE IN PRESS

INTRODUCTION

Microtubules are composed of α/β-tubulin heterodimers that coordinate diverse cellular functions including mitosis, motility, polarization, and intracellular transport (1). Being highly dynamic structures, microtubules continuously undergo polymerization and depolymerization via interactions with various motor and microtubule-associated proteins. In addition, post-translational modifications including acetylation, polyglycylation, polyglutamylation, and tyrosination/detyrosination of microtubules are essential modulators of microtubule-related functions (2). Acetylation of microtubules occurs at the lysine 40 (K40) residue of α-tubulin, a marker for stable and long-lived microtubules, that regulates cellular cargo transport, gene expression, migration, and adhesion (2, 3). The level of tubulin acetylation is regulated by the balance among the activities of histone deacetylase 6 (HDAC6), NAD-dependent deacetylase sirtuin 2 (SIRT2), and α-tubulin acetyltransferase 1 (α-TAT1/MEC-17), a major acetyltransferase (4). Since the discovery of α-TAT1, several studies have focused on clarifying its structural characterization to understand its fundamental role (5). Moreover, lysine 56 and 146 (K56 and 146) are close to the acetyl-CoA binding site, suggesting that these residues might act as mediators for the transfer of acetyl groups to α-tubulin (6). Although the N-terminal domain of α-TAT1 as a catalytic subunit is comparatively well known, the role of its C-terminal domain remains elusive. Phosphorylation at serine 237 (S237) of α-TAT1 by TGF-β-activated kinase 1 (TAK1) increases the acetyl-transferase activity upon TGF-β stimulation (7). Additionally, adenosine monophosphate–activated protein kinase phosphorylates α-TAT1 under oxidative stress, resulting in high levels of microtubule acetylation (8). These results imply that α-TAT1 activation may be controlled via phosphorylation by an upstream kinase.

Microtubule acetylation is closely associated with various diseases, including cancer, fibrotic diseases, and neurodegenerative diseases, such as Parkinson's and Alzheimer's diseases (9-11). Proinflammatory cytokines are important in the pathophysiology of various

UNCORRECTED PROOF

diseases (12). Interestingly, TGF-β, reactive oxygen species, and lipopolysaccharides act as inducers of inflammation signaling and commonly increase the acetylation of microtubules (7, 8, 13). Incident increase in microtubule acetylation by inflammation signaling may offer a fertile environment to break out of pathogenesis, resulting in the loss of neuronal cell structure and function. Therefore, targeting microtubule acetylation induced by inflammatory signals in normal tissues may be a new strategy for overcoming neurodegenerative diseases.

Casein kinase 2 (CK2) is ubiquitously expressed and highly conserved in eukaryotic cells. It is composed of two catalytic subunits (α and α') and two regulatory β-subunits that form a hetero-tetrameric structure (14). Accumulating evidence suggests that CK2 is involved in a wide variety of cellular processes including cell cycle, apoptosis, and signal transduction (15). CK2 is also associated with the regulation of microtubule reorganization. CK2 catalytic subunits (α and α') bind to tubulin and modulate microtubule dynamics and stabilization (16). Moreover, CK2 directly interacts with HDAC6 and phosphorylates S458, resulting in the activation of its deacetylase activity (17). Although the role of CK2 in microtubule function remains controversial, these findings suggest that CK2 is involved in the regulation of microtubule cytoskeletal dynamics.

We have previously reported that microtubule acetylation of fibroblasts cultured on a soft matrix that mimics normal tissue rigidity is specifically increased upon TGF-β stimulation. However, the molecular mechanism by which α-TAT1 is activated under soft matrix conditions remains unknown. In this study, we investigated the α-TAT1 activation mechanism by using a soft matrix that mimics the mechanical properties of normal tissues. We found that the C-terminus of α-TAT1 interacts with CK2α. Point mutation of putative phosphorylation sites by CK2 further revealed that the serine residue in the 236th amino acid likely regulates α-TAT1 activation via phosphorylation by CK2 in the soft matrix. Collectively, our results suggested

UNCORRECTED PROOF

that CK2 targeting can be considered a key strategy for microtubule acetylation-targeted therapies for diseases affecting soft tissues such as the brain.

UNCORRECTED PROOF

RESULTS

Inhibition of CK2 impairs microtubule acetylation induced by TGF-β on the soft matrix

To investigate the molecular mechanisms by which TGF-β can induce microtubule acetylation of fibroblasts in a soft matrix, we first screened the kinases involved in the TGF-β–induced microtubule acetylation of fibroblasts cultured on a soft matrix using diverse pharmacological inhibitors and found that the TGF-β–induced microtubule acetylation was effectively inhibited by 4,5,6,7-tetrabromobenzotriazole (TBB), a CK2 inhibitor (Fig. 1A).

To test the inhibitory effect of TBB on microtubule acetylation based on the stiffness of the matrix, cells were treated with TBB and TGF-β under various matrix mechanical conditions. As shown in Fig. 1B, the inhibition of CK2 catalytic activity by TBB notably downregulated the level of microtubule acetylation in cells cultured on a 0.5 kPa matrix. Cells cultured with blebbistatin, a myosin inhibitor, showed significant inhibition of microtubule acetylation after TBB treatment. The phosphorylation status of the signal transducer and activator of transcription 3 (STAT3) was determined to confirm the CK2 catalytic activity induced by TGF-β (15). Moreover, the formation of acetylated-α-tubulin along with elongated cells induced by TGF-β was inhibited by TBB treatment on 0.5 kPa polyacrylamide hydro-gel (PAG) (Fig. 1C). However, it only changed the cell morphology, but there was no change in the level of acetylated α-tubulin on the stiff matrix (Glass) (Fig. 1D). These results suggest that the requirement of CK2 for microtubule acetylation is dependent on the tensional status of cell-matrix interactions.

To verify the functional role of CK2 in the TGF-β–induced microtubule acetylation in the soft matrix, we generated a CK2α (catalytic subunit of CK2) knockout cell line (CK2α KO) using the clustered regularly interspaced palindromic repeat-caspase 9 (CRISPR-Cas9) system (Supplementary Fig. 1A-C). In the wild-type (WT) cells, microtubule acetylation is markedly downregulated on the soft matrix upon TGF-β stimulation in CK2α KO cells compared with

UNCORRECTED PROOF

that on the stiff matrix (Fig. 1E). Furthermore, CK2α KO mouse embryonic fibroblasts (MEFs) showed a significant reduction in the projected cell area upon TGF-β stimulation of the soft matrix (Fig. 1F). Taken together, these results show that the catalytic activity of CK2 is required for the TGF-β–induced microtubule acetylation in cells cultured on a soft matrix.

CK2 specifically interacts with α-TAT1 under low tension status

To provide insight into the underlying mechanism by which CK2 regulates microtubule acetylation, we first performed immunoprecipitation (IP) experiments using the cells transfected with Flag-CK2α and green fluorescent protein (GFP)-α-TAT1 to demonstrate the association between CK2α and α-TAT1. Fig. 2A and B show that CK2α can interact with α-TAT1. As shown in Fig. 1B, the downregulation of microtubule acetylation by CK2α inhibitor was predominant in cells on the soft matrix (0.5 kPa) and under low tension status of the cell-matrix interaction (blebbistatin) (Fig. 1B). We examined whether the binding of CK2α and α-TAT1 is dependent on the tensional status of the cell. Compared with mock-treated cells, the binding of CK2α and α-TAT1 was predominant under blebbistatin treatment (Fig. 2C). Cellular localization of α-TAT1 and CK2α by immunostaining also showed that Flag-CK2α was dispersed in the cytosol, whereas α-TAT1 was localized in the tubules and its colocalization was rarely partial. Interestingly, both proteins in the cells cultured with blebbistatin exhibited colocalization with an elongated cell axis (Fig. 2D). Taken together, these results indicate that the interaction of CK2α and α-TAT1 occurs under the low tension status of cells, such as in the soft matrix.

CK2α binds to the C-terminal domain of α-TAT1 to regulate its acetyltransferase activity

Next, we generated truncated mutants of α-TAT1 to dissect the functional domain of the α-TAT1-CK2α interaction (Fig. 3A). For α-TAT1, we constructed two truncated mutants: one

UNCORRECTED PROOF

was the C-terminal-deleted mutant (GFP-α-TAT1$^{\Delta C}$) that retained its catalytic activity, and the other was a catalytic domain–deleted mutant that only had a C-terminal domain (GFP-α-TAT1$^{\Delta N}$). Co-immunoprecipitation (Co-IP) assay showed that CK2α specifically interacted with the C-terminal domain of α-TAT1 (Fig. 3B).

Given these results, we expected that the C-terminal domain of α-TAT1 (GFP-α-TAT1$^{\Delta N}$) would act as a dominant-negative inhibitor by competing with WT α-TAT1 for binding to CK2α. Transient overexpression of the GFP-α-TAT1$^{\Delta N}$ construct significantly inhibited the interaction between α-TAT1^{WT} and CK2α by approximately 60%, but the N-terminal domain of α-TAT1 (GFP-α-TAT1$^{\Delta C}$) did not affect this interaction (Fig. 3C).

The C-terminal domain of α-TAT1 functions as a regulatory region via phosphorylation of TAK1 (7). Thus, we speculated that the interaction of CK2α with the C-terminus of α-TAT1 enables the control of its acetyltransferase activity. GFP-α-TAT1^{WT}, GFP-α-TAT1$^{\Delta C}$, and GFP-α-TAT1$^{\Delta N}$ constructs were overexpressed in the α-TAT1 KO MEFs, and the level of microtubule acetylation induced by TGF-β was analyzed. Western blotting results showed that GFP-α-TAT1$^{\Delta C}$ expression significantly reduced microtubule acetylation even though CK2 activity was increased by TGF-β (based on the level of STAT3 phosphorylation) (Fig. 3D), suggesting that the C-terminal domain of α-TAT1 controls its acetyltransferase activity via interaction with CK2α.

Next, we examined whether the overexpression of the C-terminal domain of α-TAT1 causes a decrease in microtubule acetylation upon TGF-β stimulation, as the C-terminal domain of α-TAT1 acts as a dominant-negative inhibitor by competing with α-TAT1 for binding to CK2α. Cells overexpressing the Myc-tagged C-terminal of α-TAT1 (α-TAT1$^{\Delta N}$-Myc) in WT MEFs showed shortened dendritic extensions with a lack of microtubule acetylation upon TGF-β stimulation compared to that in the mock-transfected cells under blebbistatin treatment (Fig. 3E). Taken together, these results indicate that the interaction of CK2α with the C-terminal

UNCORRECTED PROOF

domain of α-TAT1 and is crucial for the regulation of α-TAT1 acetyltransferase activity by TGF-β in the soft matrix.

Phosphorylation of α-TAT1 at S236 by CK2 is essential for the acetyltransferase activity

We found that the C-terminus of α-TAT1 contains various putative phosphorylation sites (Supplementary Fig. 2). We attempted to determine the putative phosphorylation sites that are critical for the regulation of microtubule acetylation on the soft matrix. First, we divided the C-terminus of α-TAT1 into three clusters (Cluster 1: 315–421 aa, Cluster 2: 261–314 aa, and Cluster 3: 211–260 aa) based on the closely located putative phosphorylation sites and generated truncated mutants (Fig. 4A). Although the level of microtubule acetylation was decreased in α-TAT1 KO MEFs expressing all truncated mutants compared with that observed in WT α-TAT1-expressing cells, the expression levels of GFP-α-TAT1$^{\Delta C1}$, and GFP-α-TAT1$^{\Delta C1,2}$ likely increased microtubule acetylation by TGF-β stimulation. Notably, overexpression of GFP-α-TAT1$^{\Delta C(\Delta C1\text{-}3)}$ in α-TAT1 KO MEFs failed to increase microtubule acetylation (Fig. 4A). Based on this result, we expected that the putative phosphorylation sites in Cluster 3 might be responsible for the regulation of α-TAT1 acetyltransferase activity induced by TGF-β under soft matrix conditions.

After speculating that the overall reduction in microtubule acetylation in the samples that expressed every C-terminal deleted construct of α-TAT1 (Fig. 3D) was due to structural problems or low binding affinity with polymerized microtubules, we generated another α-TAT1 mutant by deleting the Cluster 3 region alone (GFP-α-TAT1$^{\Delta C3}$). Interestingly, α-TAT1 KO MEFs expressing GFP-α-TAT1$^{\Delta C3}$ did not induce microtubule acetylation upon TGF-β stimulation and did not affect the basal level of acetyltransferase activity (Fig. 4B). α-TAT1 with deleted Cluster 3 maintained its binding affinity to polymerized microtubules compared with the WT α-TAT1. However, GFP-α-TAT1$^{\Delta C1}$ dramatically reduced the microtubule binding

UNCORRECTED PROOF

affinity to ~65%, which was consistent with a decrease in the basal level of microtubule acetylation when Cluster 1 was deleted (Supplementary Fig. 3). These results show that Cluster 3 (211–260 aa) of α-TAT1 may be required for the regulatory function of its acetyltransferase activity following TGF-β stimulation.

Cluster 3 had three putative serine phosphorylation sites (236, 237, and 238), which were highly conserved between the mouse and human species (Supplementary Fig. 4). To determine which serine residue is critical for the induction of microtubule acetylation by TGF-β, we constructed α-TAT1 mutants by substituting S236, S237, and S238 residues with alanine (S236A, S237A, and S238A, respectively) via site-directed mutagenesis. Western blotting results showed that TGF-β suppressed the acetylation of microtubules when they expressed the GFP-α-TAT1 S236A mutant instead of other alanine mutants (Fig. 4C), suggesting that phosphorylation of S236 of α-TAT1 promotes microtubule acetylation upon TGF-β stimulation.

UNCORRECTED PROOF

ARTICLE IN PRESS

DISCUSSION

α-TAT1 was first identified as a major acetyltransferase over a decade ago; however, the regulatory mechanism of its enzymatic activity is still not fully understood. In this study, we demonstrated that CK2α binds to the C-terminal domain of α-TAT1. Moreover, the substitution of serine at the 236th position, one of the serine residues that may be phosphorylated by CK2~~α~~, at the C-terminus of α-TAT1 with alanine did not cause microtubule acetylation. Although we could not confirm whether CK2 directly phosphorylated S236 of α-TAT1, these results suggest the possibility of CK2 controlling the activity of α-TAT1.

CK2 is well known for its intracellular functions through the phosphorylation of proteins related to actin rearrangement (18, 19). For example, phosphorylation of cortactin by CK2 leads to the formation of an actin-related protein 2/3 complex, which regulates actin-based invadopodia formation for tumor progression (18). However, in the case of a soft matrix, actin-related signaling is not abundant due to the lack of integrin-mediated actomyosin activity; instead, microtubule lattices function as signaling mediators (20, 21). Meanwhile, the regulatory mechanism of microtubule dynamics in the soft matrix is well defined. In this study, we demonstrated that the requirement of CK2 for microtubule acetylation is limited to the soft matrix. Inhibition of CK2 activity with TBB caused changes in the cell morphology on stiff matrix but did not affect the level of microtubule acetylation, whereas treatment with TBB completely downregulated microtubule acetylation in the cells cultured on a soft matrix. Therefore, our results suggest that CK2 may be a critical regulator of microtubule dynamics by controlling α-TAT1 activity in a soft matrix.

α-TAT1 stochastically enters the microtubule ends to transfer the acetyl group to α-tubulin. Coombes *et al.* demonstrated that α-TAT1 enters the microtubule lumen through the microtubule ends and bends or breaks in the lattice by mechanical shearing (22). Additionally, the binding affinity between α-TAT1 and its binding sites is critical for determining its mobility

UNCORRECTED PROOF

within the microtubule lumen. Kalebic *et al*. suggested that the autoacetylation of α-TAT1 at K56, 146, 210, and 221 is essential for its catalytic activity (23). Although we propose that the acetyltransferase activity of α-TAT1 is also controlled by phosphorylation of S236 at the C-terminal domain, the mechanism by which the phosphorylation of α-TAT1 could increase microtubule acetylation remains elusive. We suppose that the phosphorylation of α-TAT1 by CK2 occurs in the cytosol or outside the microtubules considering the localization of CK2. Therefore, it could be possible that the phosphorylation of α-TAT1 allow it to increase the binding affinity with the microtubule lattice, which need to be elucidated.

Although the role of microtubule acetylation in neurodegenerative diseases, such as Alzheimer's and Parkinson's diseases, remains controversial, the level of microtubule acetylation has been reported to increase in oxidative stress environments, such as neuroinflammation (11, 24, 25). In addition, this increase is required for breast cancer progression and involved in forming an active tumor microenvironment through the modulation of myofibroblast differentiation (26, 27). Microtubules function as a track where vesicle trafficking can be modulated. Acetylated microtubules preferentially recognize the kinesin-1 motor protein, thereby promoting the exocytosis of exosomes and various cytokines through polarized vesicle trafficking caused by the enhanced binding and motility of kinesin (28). These findings suggest the potential of modulating microtubule acetylation for breast cancer and neurodegenerative disease therapy. The pharmacological inhibitors of α-TAT1 have been identified, but they are yet to be fully explored (29). Therefore, α-TAT1 activity can be effectively controlled by using the CK2 inhibitor in a soft matrix mimicking the stiffening of normal tissues; this result is meaningful because it serves as a basis for developing a new bypass strategy to control microtubule acetylation.

Taken together, we have demonstrated through this research that the acetylation of microtubules increased in soft matrix can be effectively blocked through downregulation of

UNCORRECTED PROOF

CK2 activity. Thus, it is expected to present a new treatment method for malignant tumors or brain diseases such as Alzheimer's Disease occurring in a mechanical and soft matrix environment.

UNCORRECTED PROOF

MATERIALS AND METHODS

Materials and methods are available in the supplemental material.

UNCORRECTED PROOF

ARTICLE IN PRESS

ACKNOWLEDGMENTS

This research was supported by grants from the National Research Foundation of Korea (NRF) funded by the Korean government (MSIT) (NRF-2020R1A2C2007389) and the Chung-Ang University Research Grant (2020).

UNCORRECTED PROOF

ARTICLE IN PRESS

CONFLICTS OF INTEREST

The authors declare that they have no conflicts of interest.

UNCORRECTED PROOF

FIGURE LEGENDS

Fig. 1. Casein kinase 2 (CK2) is required for the transforming growth factor (TGF)-β–induced microtubule acetylation on the soft matrix. (A and B) Mouse embryonic fibroblasts (MEFs) were seeded on fibronectin (10 ug/mL)-coated ~0.5 kPa polyacrylamide gel (PAG) in a plastic culture dish with or without TGF-β (2 ng/mL), 4,5,6,7-tetrabromobenzotriazole (TBB) (10 μM), and blebbistatin (10 μM). After 8 h of incubation, protein lysates obtained from individual conditions were subjected to western blotting with the indicated antibodies. **(C and D)** Immunocytochemistry of MEFs seeded on fibronectin-coated ~0.5 kPa PAG and coverslips with or without TGF-β (2 ng/mL) and TBB (10 μM) for 8 h. Graphs show the projected cell area of 30 cells randomly incubated on ~0.5 kPa PAGs and coverslips. Statistical significance was determined via one-way analysis of variance (ANOVA) with Tukey's post hoc test. Projected cell area; one-way ANOVA, $F_{3,116} = 75.84$. ***$p < 0.005$, n.s. not significant. Scale bar, 25 μm. For each value, measurements were made on 30 randomly photographed cells. **(E)** Wild-type (WT) and CK2α knockout (KO) MEFs were seeded on 0.5 kPa PAG in a plastic culture dish upon TGF-β stimulation for 8 h. **(F)** Measurement of projected cell area of WT and CK2α KO MEFs on ~0.5 kPa PAGs (n = 30, each group). Statistical significance was determined via one-way ANOVA with Tukey's post hoc test. Projected cell area; one-way ANOVA, $F_{3,116} = 42.02$. ***$p < 0.005$, n.s. not significant. For each value, measurements were made on 30 randomly photographed cells.

Fig. 2. CK2α strongly binds to α-tubulin acetyltransferase 1 (α-TAT1) on the soft matrix. (A and B) Co-immunoprecipitation (co-IP) assay was performed to analyze the interaction between Flag-CK2α and green fluorescent protein (GFP)-α-TAT1 in HEK293T cells. **(C)** Co-IP assay was performed to analyze the interaction between Flag-CK2α and GFP-α-TAT1 with

UNCORRECTED PROOF

or without blebbistatin in WT MEFs. **(D)** Cellular localization of Flag-CK2α and GFP-α-TAT1 in MEFs with or without blebbistatin was observed via immunocytochemistry using anti-FLAG antibodies. White arrows indicate the colocalization of Flag-CK2α and GFP-α-TAT1. Scale bars: 25 μm and 5 μm (cropped image). Graphs show the fluorescence intensities of Flag-CK2α (red) and GFP-α-TAT1 (green).

Fig. 3. C-terminal domain of α-TAT1 is essential for the regulation of its acetyltransferase activity. (A) Schematic representation of GFP-α-TAT1^{WT} (1–421 aa), GFP-α-TAT1$^{\Delta C}$ (1–211 aa), GFP-α-TAT1$^{\Delta N}$ (190–421 aa), and α-TAT1$^{\Delta N}$-Myc (190–421 aa). **(B)** HEK293T cells were transfected with the indicated plasmids, and co-IP was performed with anti-mouse IgG and anti-Flag antibodies. **(C)** Co-IP assay shows the binding affinities of Flag-CK2α and GFP-α-TAT1 by overexpression of GFP-α-TAT1$^{\Delta C}$ and GFP-α-TAT1$^{\Delta N}$. **(D)** α-TAT1 KO MEFs were transfected with GFP-C1, GFP-α-TAT1^{WT}, GFP-α-TAT1$^{\Delta C}$, and GFP-α-TAT1$^{\Delta N}$ and treated with TGF-β and blebbistatin. Lysates from cells were subjected to western blotting with the indicated antibodies **(E)** WT MEFs were overexpressed with Myc-empty vector or α-TAT1$^{\Delta N}$-Myc and treated with blebbistatin and/or TGF-β. Next, the cells were fixed and immunostained with anti-Myc and anti-acetylated α-tubulin antibodies. The number of cells having dendrites whose lengths were more or less than two-times the lengths of their cell bodies were counted. For each value, measurements were made on 50 randomly photographed cells. White arrows indicate the long tail-like dendrites. Scale bar, 50 μm.

Fig. 4. Phosphorylation of α-TAT1 at S236 regulates the TGF-β–induced microtubule acetylation. (A and B) The C-terminal domain (190–421 aa) is divided into three clusters, and each cluster and mutants with deleted Cluster 3 region are indicated. α-TAT1 KO MEFs were transfected with the indicated plasmids and treated with blebbistatin and/or TGF-β for 8 h.

UNCORRECTED PROOF

Graphs show the relative band intensity of acetylated-α-tubulin. Biological significance of the acetylated α-tubulin levels in α-TAT1 KO MEFs by TGF-β was assessed using Student's *t*-test and compared with that of the control. **p* < 0.05, ***p* < 0.01, ****p* < 0.005, n.s. not significant. **(C)** α-TAT1 and its mutants, in which the conserved serine residues (S) (S236, S237, and S238) were mutated to alanine (A) (S236A, S237A, S238A and S237/238A). α-TAT1 KO MEFs were transfected with the indicated mutants, and the level of acetylated-α-tubulin upon TGF-β stimulation was determined.

UNCORRECTED PROOF

ARTICLE IN PRESS

REFERENCES

1. Garcin C and Straube A (2019) Microtubules in cell migration. Essays Biochem 63, 509-520
2. Westermann S and Weber K (2003) Post-translational modifications regulate microtubule function. Nat Rev Mol Cell Biol 4, 938-947
3. Balabanian L, Berger CL and Hendricks AG (2017) Acetylated Microtubules Are Preferentially Bundled Leading to Enhanced Kinesin-1 Motility. Biophys J 113, 1551-1560
4. Janke C and Montagnac G (2017) Causes and Consequences of Microtubule Acetylation. Curr Biol 27, R1287-R1292
5. Al-Bassam J and Corbett KD (2012) alpha-Tubulin acetylation from the inside out. Proc Natl Acad Sci U S A 109, 19515-19516
6. Taschner M, Vetter M and Lorentzen E (2012) Atomic resolution structure of human alpha-tubulin acetyltransferase bound to acetyl-CoA. Proc Natl Acad Sci U S A 109, 19649-19654
7. Shah N, Kumar S, Zaman N et al (2018) TAK1 activation of alpha-TAT1 and microtubule hyperacetylation control AKT signaling and cell growth. Nat Commun 9, 1696
8. Mackeh R, Lorin S, Ratier A et al (2014) Reactive oxygen species, AMP-activated protein kinase, and the transcription cofactor p300 regulate alpha-tubulin acetyltransferase-1 (alphaTAT-1/MEC-17)-dependent microtubule hyperacetylation during cell stress. J Biol Chem 289, 11816-11828
9. Ko P, Choi JH, Song S et al (2021) Microtubule Acetylation Controls MDA-MB-231 Breast Cancer Cell Invasion through the Modulation of Endoplasmic Reticulum Stress. Int J Mol Sci 22
10. You E, Huh YH, Kwon A et al (2017) SPIN90 Depletion and Microtubule Acetylation Mediate Stromal Fibroblast Activation in Breast Cancer Progression. Cancer Res 77, 4710-4722
11. Cappelletti G, Calogero AM and Rolando C (2021) Microtubule acetylation: A reading key to neural physiology and degeneration. Neurosci Lett 755, 135900
12. Friedrich M, Pohin M and Powrie F (2019) Cytokine Networks in the Pathophysiology of Inflammatory Bowel Disease. Immunity 50, 992-1006
13. Wang B, Rao YH, Inoue M et al (2014) Microtubule acetylation amplifies p38 kinase signalling and anti-inflammatory IL-10 production. Nat Commun 5, 3479
14. Graham KC and Litchfield DW (2000) The regulatory beta subunit of protein kinase CK2 mediates formation of tetrameric CK2 complexes. J Biol Chem 275, 5003-5010
15. Borgo C, D'Amore C, Sarno S, Salvi M and Ruzzene M (2021) Protein kinase CK2: a potential therapeutic target for diverse human diseases. Signal Transduct Target Ther 6, 183
16. Lim AC, Tiu SY, Li Q and Qi RZ (2004) Direct regulation of microtubule dynamics by protein kinase CK2. J Biol Chem 279, 4433-4439
17. Watabe M and Nakaki T (2011) Protein kinase CK2 regulates the formation and clearance of aggresomes in response to stress. J Cell Sci 124, 1519-1532
18. Markwell SM, Ammer AG, Interval ET et al (2019) Cortactin Phosphorylation by Casein Kinase 2 Regulates Actin-Related Protein 2/3 Complex Activity, Invadopodia Function, and Tumor Cell Invasion. Mol Cancer Res 17, 987-1001
19. Xavier CP, Rastetter RH, Blomacher M et al (2012) Phosphorylation of CRN2 by CK2 regulates F-actin and Arp2/3 interaction and inhibits cell migration. Sci Rep 2, 241

UNCORRECTED PROOF

20. Rhee S, Jiang H, Ho CH and Grinnell F (2007) Microtubule function in fibroblast spreading is modulated according to the tension state of cell-matrix interactions. Proc Natl Acad Sci U S A 104, 5425-5430
21. Bouchet BP and Akhmanova A (2017) Microtubules in 3D cell motility. J Cell Sci 130, 39-50
22. Coombes C, Yamamoto A, McClellan M et al (2016) Mechanism of microtubule lumen entry for the alpha-tubulin acetyltransferase enzyme alphaTAT1. Proc Natl Acad Sci U S A 113, E7176-E7184
23. Kalebic N, Martinez C, Perlas E et al (2013) Tubulin acetyltransferase alphaTAT1 destabilizes microtubules independently of its acetylation activity. Mol Cell Biol 33, 1114-1123
24. Cartelli D, Ronchi C, Maggioni MG, Rodighiero S, Giavini E and Cappelletti G (2010) Microtubule dysfunction precedes transport impairment and mitochondria damage in MPP+ -induced neurodegeneration. J Neurochem 115, 247-258
25. Mao CX, Wen X, Jin S and Zhang YQ (2017) Increased acetylation of microtubules rescues human tau-induced microtubule defects and neuromuscular junction abnormalities in Drosophila. Dis Model Mech 10, 1245-1252
26. You E, Ko P, Jeong J et al (2020) Dynein-mediated nuclear translocation of yes-associated protein through microtubule acetylation controls fibroblast activation. Cell Mol Life Sci 77, 4143-4161
27. Boggs AE, Vitolo MI, Whipple RA et al (2015) alpha-Tubulin acetylation elevated in metastatic and basal-like breast cancer cells promotes microtentacle formation, adhesion, and invasive migration. Cancer Res 75, 203-215
28. Reed NA, Cai D, Blasius TL et al (2006) Microtubule acetylation promotes kinesin-1 binding and transport. Curr Biol 16, 2166-2172
29. Kwon A, Lee GB, Park T et al (2020) Potent Small-Molecule Inhibitors Targeting Acetylated Microtubules as Anticancer Agents Against Triple-Negative Breast Cancer. Biomedicines 8

UNCORRECTED PROOF

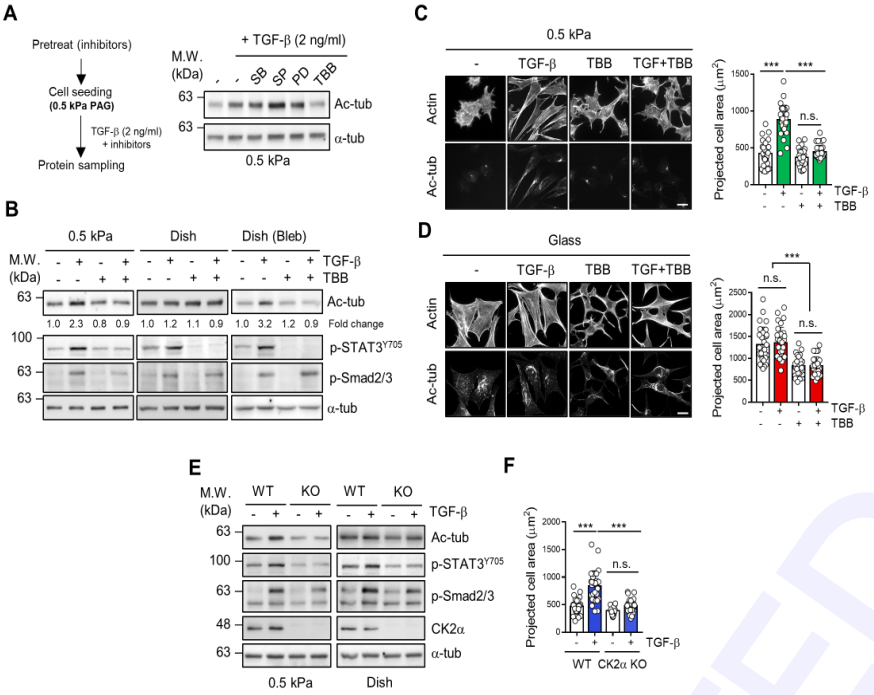

Fig.1
(You *et al.*)

Fig. 1.

UNCORRECTED PROOF

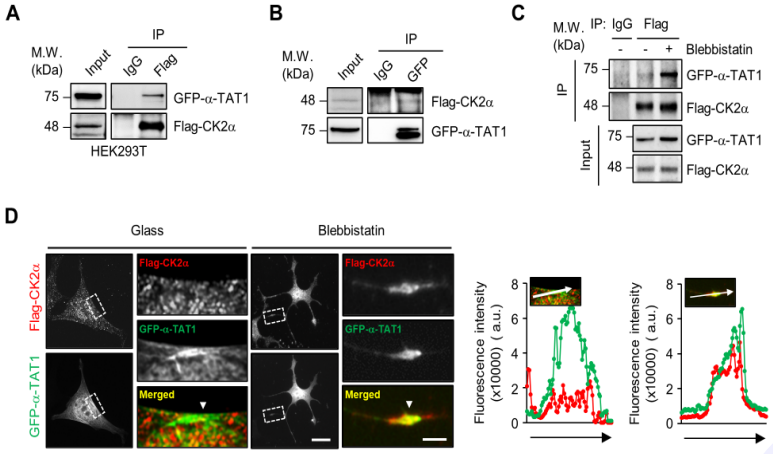

Fig.2
(You *et al.*)

Fig. 2.

UNCORRECTED PROOF

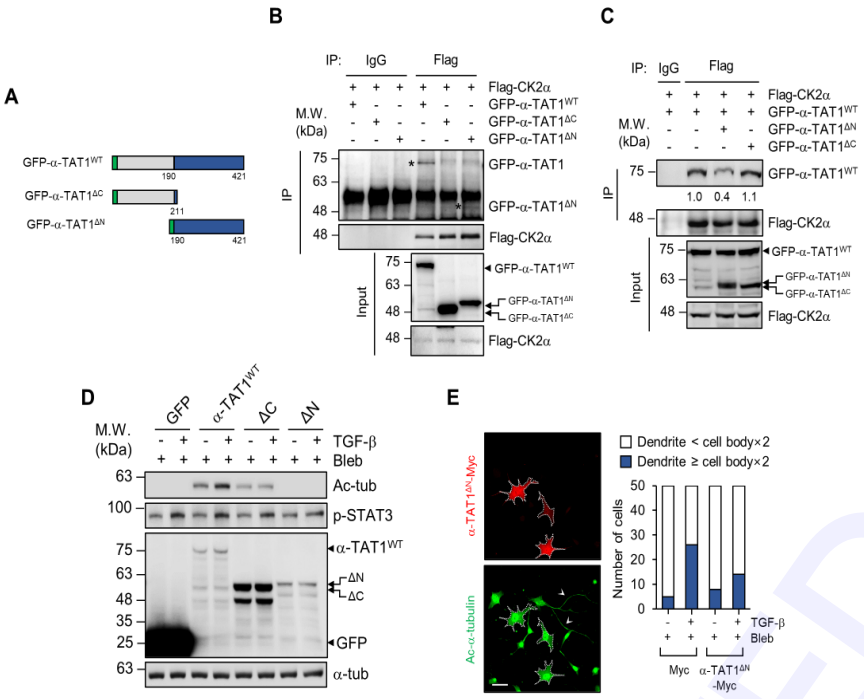

Fig.3
(You *et al.*)

Fig. 3.

UNCORRECTED PROOF

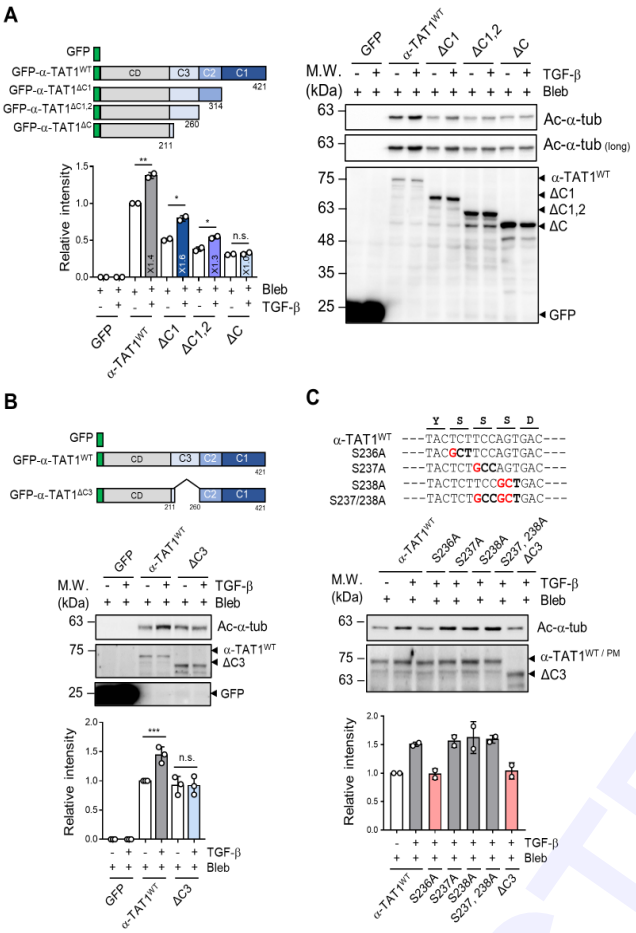

Fig.4
(You *et al.*)

Fig. 4.

UNCORRECTED PROOF

ARTICLE IN PRESS

Manuscript Type: Article

Title: Casein kinase 2 promotes the TGF-β–induced activation of α-tubulin acetyltransferase 1 in fibroblasts cultured on a soft matrix

Authors' names: Eunae You[1§], Jangho Jeong[1§], Jieun Lee[1], Seula Keum[1], Ye Eun Hwang[1], Jee-Hye Choi[1*] and Sangmyung Rhee[1*]

Affiliation: [1]Department of Life Science, Chung-Ang University, Seoul, 06974, Republic of Korea

[§]These authors contributed equally to this work.

Running Title: Regulation of α-TAT1 activity by CK2

Keywords: TGF-β, Casein kinase 2, Microtubule acetylation, α-tubulin acetyltransferase 1, Extracellular matrix

Corresponding Authors' Information:

Sangmyung Rhee

Tel: +82-2-820-5818; Fax: +82-2-825-5206; E-mail: sangmyung.rhee@cau.ac.kr

Jee-Hye Choi

Tel: +82-2-814-3997; Fax: +82-2-825-5206; E-mail: choijh97@cau.ac.kr

UNCORRECTED PROOF

MATERIALS AND METHODS

Antibodies and reagents

Primary antibodies were obtained against the following proteins: acetylated α-tubulin (#5335), phospho-STAT3^{Y705} (#9131), and phopho-Smad2$^{S465/467}$/Smad3$^{S423/425}$ (#8828; Cell signaling Technology, MA, USA); GFP (sc-9996), α-tubulin (#sc-12462), and CK2α (#sc-12738; Santa Cruz Biotechnology, CA, USA). Moreover, Flag M2 antibody (#3165) was purchased from Sigma-Aldrich (MO, USA), whereas horseradish peroxidase (HRP)–conjugated goat anti-mouse (115-035-006) and HRP-conjugated goat anti-rabbit (111-035-006) antibodies were purchased from Jackson ImmunoResearch Laboratories (PA, USA). We also purchased blebbistatin (#B592500; Toronto Research Chemicals, ON, Canada), TGF-β1 (#240B; R&D systems, MN, USA), TBB (#218697; Calbiochem, CA, USA), SB202190 (#S7067; Sigma-Aldrich), SP600125 (#S5567; Sigma-Aldrich), and PD98059 (#1213, MEK inhibitor; Tocris, Bristol, UK).

Plasmid constructs

Various truncated mutants of α-TAT1 (*Mus musculus*, isoform 1) tagged with GFP or Myc were generated by polymerase chain reaction (PCR) using specific forward and reverse primers complementary to the defined sequences, using GFP-α-TAT1 as a template. α-TAT1$^{\Delta C}$, α-TAT1$^{\Delta N}$, α-TAT1$^{\Delta C1}$, α-TAT1$^{\Delta C1\text{-}2}$, and α-TAT1$^{\Delta C3}$ were cloned between XhoI and BamHI restriction sites and inserted into the pEGFP-C1 vector (Clontech, CA, USA). α-TAT1$^{\Delta N}$ was cloned between BamHI and XbaI restriction sites and inserted into the pcDNA6/Myc-His A vector (Invitrogen). *Csnk2a1* (CK2α) cDNA was amplified from XE242 mouse CK2α CS2p+ (#16730; Addgene, MA, USA) via PCR and cloned into the p3xFLAG-CMV™-10 expression vector (#E4401; Sigma-Aldrich). The primer sequences used for plasmid construction are listed in Supplementary Table 1. Point mutations were introduced via PCR using the *PfuUltra* High-

UNCORRECTED PROOF

Fidelity DNA polymerase (#600380; Agilent, CA, USA). The sequences of the primers used for site-directed mutagenesis are listed in Supplementary Table 2.

Cell culture

WT and α-TAT1 KO MEFs were cultured in Dulbecco's modified Eagle's medium (DMEM; Gibco-BRL, Grand Island, NY, USA) supplemented with 1% GlutaMAX, 1% minimum essential medium (MEM) containing non-essential amino acids, 10% fetal bovine serum (FBS) (Youngin Frontier, Seoul, Korea), 100 unit/mL penicillin, and 100 ug/mL streptomycin (Welgene, Seoul, Korea). The cells were maintained at 37 °C and 5% carbon dioxide in a humidified incubator. HEK293T cells were obtained from American Type Culture Collection (Manassas, VA, USA). HEK293T cells were cultured in DMEM supplemented with 10% FBS.

Generation of CK2α KO cell line using CRISPR/Cas9

A 20-bp guide RNA (gRNA) sequence (5′-AGACATTGTAAAAGACCCTG-3′) targeting genomic DNA within exon 3 of *CK2α* was selected from the GenBank database (Accession number NC_000068; region: 152067851–152123772) of predicted high-specificity protospacer adjacent motif sequences in the mouse exome. gRNA was cloned into LentiCRISPR V2 (#52961; Addgene) and WT MEFs were infected with lentivirus containing the gRNA sequence with polybrene (0.8 μg/mL) for 48 h. Cells were selected using puromycin (2 μg/mL) and single-cell colonies were acquired. *CK2α* KO cell line was verified by genomic DNA sequencing and western blotting.

Transfection

The cells (3×10^5) were plated on 60-mm dishes and then transfected with 2.5 μg of DNA after 24 h using Lipofectamine 2000 (#11668019; Thermo Fisher Scientific, NH, USA), according

UNCORRECTED PROOF

to the manufacturer's instructions. Later, the cells (7 x 10^5) were plated in a 6-well plate and then transfected with 500 ng of DNA after 24 h using TransFectin™ Lipid Reagent (#1703351; Bio-Rad, CA, USA).

Co-IP and western blotting

For western blotting, the cells were lysed with the lysis buffer containing 1% Nonidet P-40 (NP-40), 1% sodium dodecyl sulfate, 150 mM NaCl, 6 mM Na_2HPO_4, 4 mM NaH_2PO_4, 2 mM ethylenediaminetetraacetic acid (EDTA), 50 mM NaF, 1 mM Na_3VO_4, 1 mM 1,4-dithiothreitol, and 1 mM phenylmethylsulfonyl fluoride (PMSF). Protein concentrations were measured using the bicinchoninic acid assay (Thermo Fisher Scientific). For IP, the cells were lysed with IP buffer (50 mM Tris-Cl (pH 7.4), 150 mM NaCl, 1% NP-40, 0.5% Triton X-100, 1 mM Na_3VO_4, 50 mM NaF, 1 mM PMSF, 10% glycerol, and 2 mM EDTA) for 1 h on ice and centrifuged at 4 °C and 13,000 rpm for 15 min to collect the supernatant. Protein concentrations were measured using Bradford assay (Bio-Rad, Hercules, CA, USA). The proteins (1 mg) were incubated with primary antibodies at 4 °C overnight. Following incubation, protein A/G beads were incubated at 4 °C for 2 h. Finally, the beads were washed thrice with the IP buffer, boiled, and analyzed by western blotting. Signals were developed using enhanced chemiluminescence reagents (Bio-Rad) and band density was measured using the Quantity One system (Bio-Rad).

Statistical analyses

Statistical analyses were performed using GraphPad Prism 7 software (GraphPad Software, CA, USA). We used the Student's *t*-test to compare two groups and one-way analysis of variance (ANOVA) to compare more than two groups. Tukey's multiple comparison test was applied to all ANOVA post hoc tests. ANOVA *F* values are described in each figure legend as $F_{(DFn,\ Dfd)}$, where DFn is the df numerator, and Dfd is the df denominator. Statistical

UNCORRECTED PROOF

significance was set at $p < 0.05$ ($^{*}p < 0.05$, $^{**}p < 0.01$, $^{***}p < 0.005$). All data are presented as the mean ± standard deviation.

UNCORRECTED PROOF

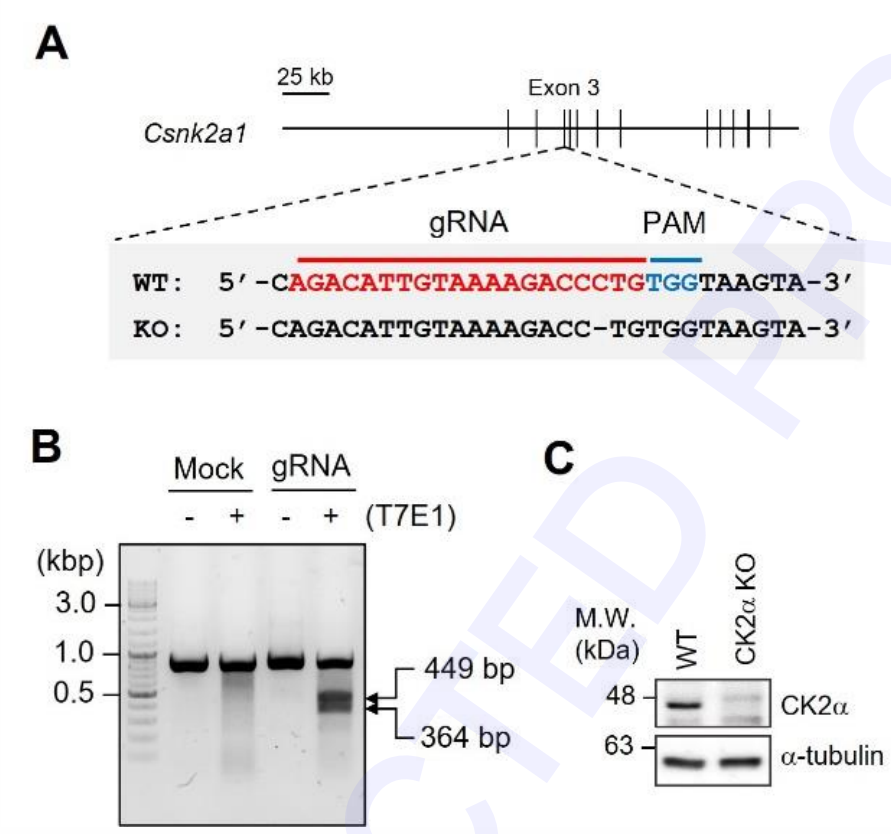

Supplementary Fig. 1. CK2α knockout (KO) cells were generated using the clustered regularly interspaced palindromic repeat-caspase 9 (CRISPR-Cas9) system. (A) Single guide RNA (gRNA) targeting exon 3 of *Csnk2a1* was selected by the GeneScript software. CK2α KO MEFs were verified via DNA sequencing (single nucleotide deletion) **(B)** T7 endonuclease 1 assay was performed to determine the efficiency of gRNA. **(C)** Protein extracts obtained from the wild-type (WT) and CK2a KO MEFs were subjected to western blotting to assess the protein expression levels of CK2α.

UNCORRECTED PROOF

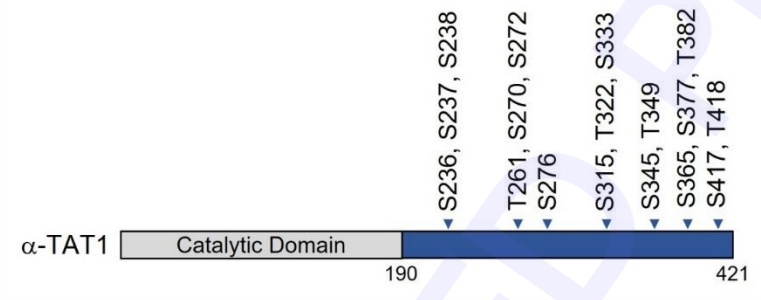

Supplementary Fig. 2. Putative phosphorylation sites in the C-terminal domain of α-tubulin acetyltransferase 1 (α-TAT1). Schematic representation of α-TAT1 of *Mus musculus*. Putative serine/threonine phosphorylation sites in the C-terminal domain are indicated. These sites were obtained from PhosphoSitePlus and Netphos 3.1.

UNCORRECTED PROOF

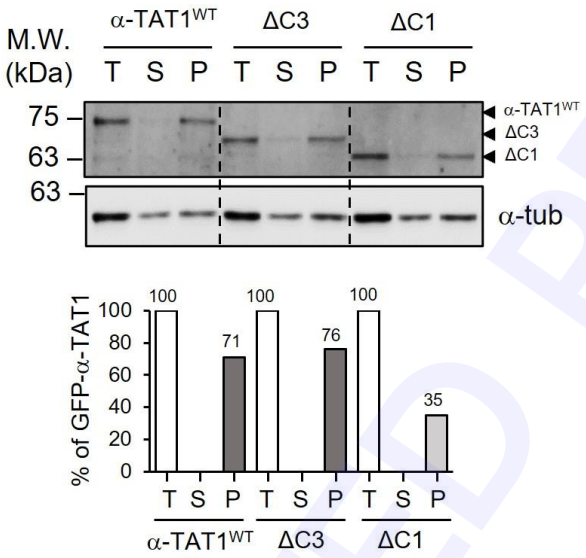

Supplementary Fig. 3. Deletion of the Cluster 3 domain of α-TAT1 maintained the binding affinity to polymerized microtubules. α-TAT1 KO MEFs were transfected with the indicated plasmids, and a microtubule sedimentation assay was conducted. Each fraction was assessed via western blotting to detect the levels of α-TAT1 constructs (WT, ΔC3, and ΔC1), supernatant (S) (depolymerized tubulin), and pellet (P) (polymerized tubulin).

UNCORRECTED PROOF

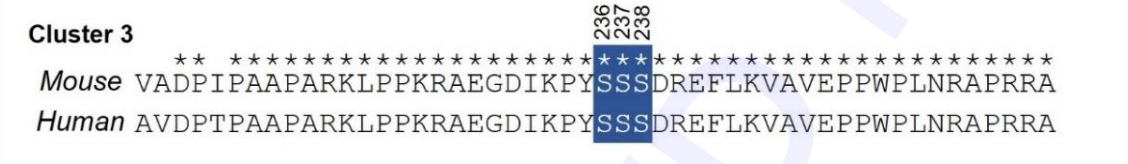

Supplementary Fig. 4. Amino acid sequence alignment of Cluster 3 in α-TAT1 between mice (*M. musculus*) and humans (*Homo sapiens*). Cluster 3 domain in α-TAT1 was highly conserved in both mice and humans.

UNCORRECTED PROOF

Supplementary Table 1. Primers used for plasmid construction

Plasmid	Direction (Restriction enzyme)	Sequence
GFP-α-TAT1$^{\Delta C1}$	F (XhoI)	CCGCTCGAGGAATGGAGTTCCCGTTCGAT
	R (BamHI)	CGGGATCCGCCTCCAGGGTCAGTGGC
GFP-α-TAT1$^{\Delta C1,2}$	F (XhoI)	CCGCTCGAGGAATGGAGTTCCCGTTCGAT
	R (BamHI)	CGGGATCCGGCACGCCGAGGGGCCCTGTT
GFP-α-TAT1$^{\Delta C}$	F (XhoI)	CCGCTCGAGGAATGGAGTTCCCGTTCGAT
	R (BamHI)	CGGGATCCCACAGCAGCACGAGAGTG
GFP-α-TAT1$^{\Delta N}$	F (XhoI)	CCGCTCGAGGAATGGCCGATCCCATACCTGCTGCT
	R (BamHI)	CGGGATCCTTACCAAGGCCTGGTGCTGCG
α-TAT1$^{\Delta N}$-Myc	F (BamHI)	CGGGATCCATGGCCGATCCCATACCTGCTGCT
	R (XbaI)	GCTCTAGACCAAGGCCTGGTGCTGCG
GFP-α-TAT1$^{\Delta C3}$	1-F (XhoI)	CCGCTCGAGGAATGGAGTTCCCGTTCGAT
	2-R	GTGGGCTGGAGGTGTCACAGCAGCACGAGA
	3-F	TCTCGTGCTGCTGTGACACCTCCAGCCCAC
	4-R (BamHI)	CGGGATCCTTACCAAGGCCTGGTGCTGCG
Flag-CK2α	F (NotI)	AAGGAAAAAAGCGGCCGCGATGTCGGGACCCGTGCCAAG
	R (KpnI)	CGGGGTACCTTACTGCTGAGCGCCAGC

UNCORRECTED PROOF

ARTICLE IN PRESS

Supplementary Table 2. Primers used for site-directed mutagenesis of α-TAT1

Plasmid	Direction	Sequence
GFP-α-TAT1 (S236A)	F	GGAGACATTAAGCCATACGCTTCCAGTGACAGAGAATTC
	R	GAATTCTCTGTCACTGGAAGCGTATGGCTTAATGTCTCC
GFP-α-TAT1 (S237A)	F	GACATTAAGCCATACTCTGCCAGTGACAGAGAATTCCTGAAG
	R	CTTCAGGAATTCTCTGTCACTGGCAGAGTATGGCTTAATGTC
GFP-α-TAT1 (S238A)	F	GACATTAAGCCATACTCTTCCGCTGACAGAGAATTCCTGAAG
	R	CTTCAGGAATTCTCTGTCAGCGGAAGAGTATGGCTTAATGTC
GFP-α-TAT1 (S237/238A)	F	GACATTAAGCCATACTCTGCCGCTGACAGAGAATTCCTGAAG
	R	CTTCAGGAATTCTCTGTCAGCGGCAGAGTATGGCTTAATGTC

UNCORRECTED PROOF